Chapter 14

The Atlantic Ocean

A glance at the distribution of high quality ocean data (Figure 2.3) tells us that the Atlantic Ocean is by far the best researched part of the world ocean. This is particularly true of the North Atlantic Ocean, the home ground of many oceanographic research institutions of the USA and Europe. We therefore have a wealth of information, and our task in describing the essential features of the Atlantic Ocean will not so much consist of finding reasonable estimates for missing data but finding the correct level of generalization from a bewildering and complex data set.

Bottom topography

Several outstanding topographic features distinguish the Atlantic Ocean from the Pacific and Indian Oceans. First of all, the Atlantic Ocean extends both into the Arctic and Antarctic regions, giving it a total meridional extent - if the Atlantic part of the Southern Ocean is included - of over 21,000 km from Bering Strait through the Arctic Mediterranean Sea to the Antarctic continent. In comparison, its largest zonal distance, between the Gulf of Mexico and the coast of north west Africa, spans little more than 8,300 km. Secondly, the Atlantic Ocean has the largest number of adjacent seas, including mediterranean seas which influence the characteristics of its waters. Finally, the Atlantic Ocean is divided rather equally into a series of eastern and western basins by the Mid-Atlantic Ridge, which in many parts rises to less than 1000 m depth, reaches the 2000 m depth contour nearly everywhere, and consequently has a strong impact on the circulation of the deeper layers.

When all its adjacent seas are included, the Atlantic Ocean covers an area of $106.6 \cdot 10^6$ km^2. Without the Arctic Mediterranean and the Atlantic part of the Southern Ocean, its size amounts to $74 \cdot 10^6$ km^2, slightly less than the size of the Southern Ocean. Although all its abyssal basins are deeper than 5000 m and most extend beyond 6000 m depth in their deepest parts (Figure 14.1), the average depth of the Atlantic Ocean is 3300 m, less than the mean depths of both the Pacific and Indian Oceans. This results from the fact that shelf seas (including its adjacent and mediterranean seas) account for over 13% of the surface area of the Atlantic Ocean, which is two to three times the percentage found in the other oceans.

Three of the features shown in Figure 14.1 deserve special mention. The first is the difference in depth east and west of the Mid-Atlantic Ridge near 30°S. The Rio Grande Rise comes up to about 650 m; but west of it the Rio Grande Gap allows passage of deep water near the 4400 m level. In contrast, the Walvis Ridge in the east, which does not reach 700 m depth, blocks flow at the 4000 m level. The second is the Romanche Fracture Zone (Figure 8.2) some 20 km north of the equator which allows movement of water between the western and eastern deep basins at the 4500 m level (its deepest part, the Romanche Deep, exceeds 7700 m depth but connects only to the western basins). Other fracture zones north of the equator have similar characteristics; but the Romanche Fracture Zone is the first opportunity for water coming from the south to break through the barrier posed by the Mid-Atlantic Ridge. The third feature is the Gibbs Fracture Zone near 53°N which allows passage of water at the 3000 m level; its importance for the spreading of Arctic Bottom Water was already discussed in Chapter 7.

Of interest from the point of view of oceanography are the sill characteristics of the five mediterranean seas. The Arctic Mediterranean Sea, which is by far the largest comprising 13% of the Atlantic Ocean area, was already discussed in Chapter 7; its sill is about 1700 km wide and generally less than 500 m deep with passages exceeding 600 m depth in Denmark Strait and 800 m in the Faroe Bank Channel. The Strait of Gibraltar, the point of communication between the Eurafrican Mediterranean Sea and the main Atlantic Ocean, spans a distance of 22 km with a sill depth of 320 m. The American Mediterranean Sea has several connections with the Atlantic Ocean basins, the major ones being east of Puerto Rico and between Cuba and Haiti where sill depths are in the vicinity of 1700 m and between Florida and the Bahamas with a sill depth near 750 m. Baffin Bay communicates through the 350 km wide Davis Strait where the sill depth is less than 600 m. Finally, communication with the Baltic Sea is severely restricted by the shallow and narrow system of passages of Skagerrak, Kattegat, Sund and Belt where the sill depth is only 18 m.

The wind regime

The information needed from the atmosphere is again included in Figures 1.2 - 1.4. An outstanding feature is the large seasonal variation of northern hemisphere winds in comparison to the low variability of the wind field in the subtropical zone of the southern hemisphere. This is similar to the situation in the Pacific Ocean and again caused by the impact of the Siberian and to a lesser extent North American land masses on the air pressure distribution. As a result the subtropical high pressure belt, which in the northern winter runs from the Florida - Bermuda region across the Canary Islands, the Azores, and Madeira and continues across the Sahara and the Eurafrican Mediterranean Sea into central Siberia, is reduced during summer to a cell of high pressure with its centre near the Azores. This is the well-known Azores High which dominates European summer weather, bringing winds of moderate strength. During winter, the contrast between cold air over Siberia and air heated by the advection of warm water in the Norwegian Current region leads to the development of the equally well-known Icelandic Low with its strong Westerlies, which follow the isobars between the subtropical high pressure belt and the low pressure to the north. The seasonal disturbance of the subtropical high pressure belt in the southern hemisphere is much less developed, and the Westerlies show correspondingly less seasonal variation there.

The Trade Winds are somewhat stronger in winter (February north of the equator and August in the south) than in summer on both hemispheres. Seasonal wind reversals of monsoon characteristics are of minor importance in the Atlantic Ocean; their occurrence is limited to two small regions, along the African coastline from Senegal to Ivory Coast and in the Florida - Bermuda area. Important seasonal change in wind direction is observed along the east coast of North America which experiences offshore winds during most of the year but warm alongshore winds in summer.

The mean wind stress distribution of the South Atlantic Ocean shows close resemblance to that of the Indian Ocean. The maximum Westerlies do not lie quite so far north as in the Indian Ocean (at about 50°S instead of 45°S), but the maximum Trade Winds occur at very similar latitudes (about 15°S, associated with somewhat smaller wind stress curls). The Doldrum belt, or Intertropical Convergence Zone (ITCZ), is found north of the equator,

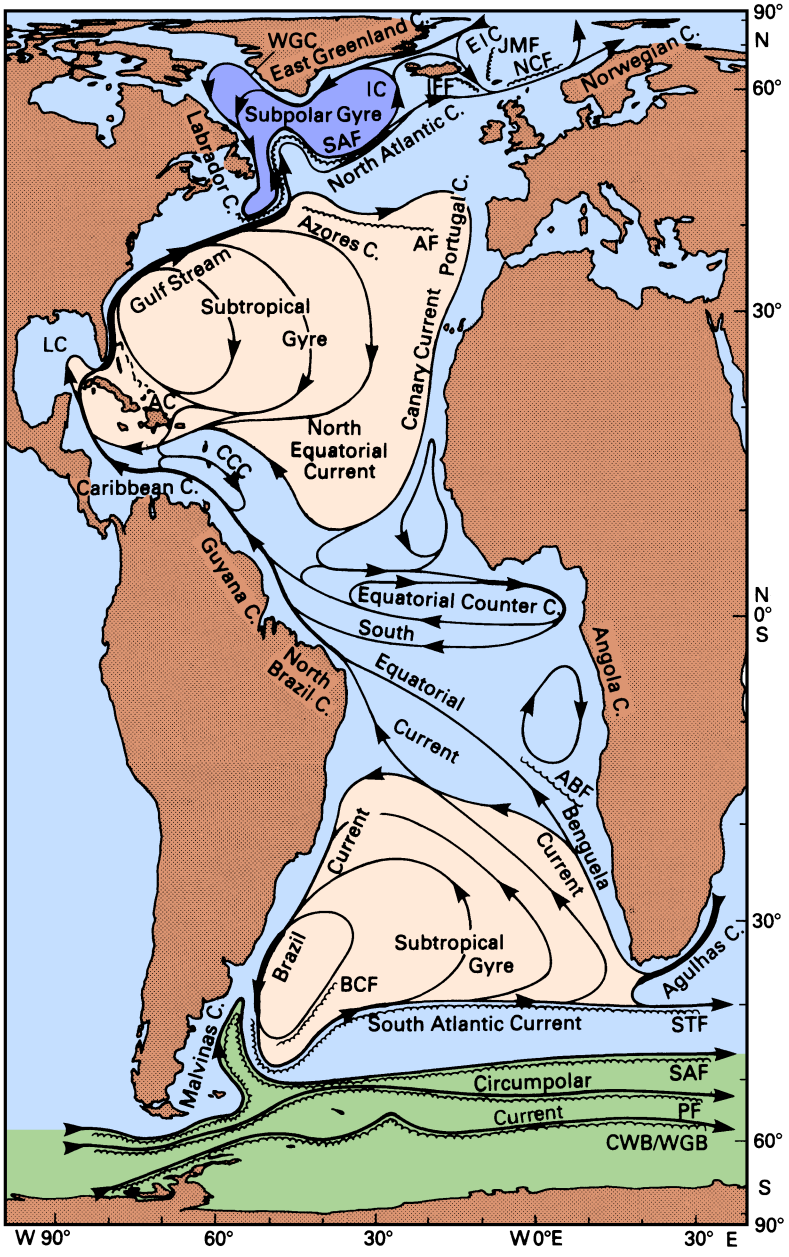

Fig. 14.2. Surface currents of the Atlantic Ocean. Abbreviations are used for the East Iceland (EIC), Irminger (IC), West Greenland (WGC), and Antilles (AC) Currents and the Caribbean Countercurrent (CCC). Other abbreviations refer to fronts: JMF: Jan Mayen Front, NCF: Norwegian Current Front, IFF: Iceland - Faroe Front, SAF: Subarctic Front, AF: Azores Front, ABF: Angola - Benguela Front, BCF: Brazil Current Front, STF: Subtropical Front, SAF: Subantarctic Front, PF: Polar Front, CWB/WGB: Continental Water Boundary / Weddell Gyre Boundary. Adapted from Duncan *et al*. (1982), Krauss (1986) and Peterson and Stramma (1991).

(SEC), again a region of broad and uniform westward flow with similar speeds, extends from about 3°N to at least 15°S. Just as in the Pacific Ocean it is interspersed with eastward flow both at the surface and below the thermocline. The *South Equatorial Countercurrent* (SECC) is weak, narrow and variable and therefore not resolved by Figure 14.5, which is based on 2° averages in latitude. It often shows maximum speed (around 0.1 m s^{-1}) below 100 m depth and is masked by weak westward flow at the surface. The *North Equatorial Undercurrent* (NEUC) and the *South Equatorial Undercurrent* (SEUC) are both narrow and swift, with maximum speeds of 0.4 m s^{-1} near 200 m depth.

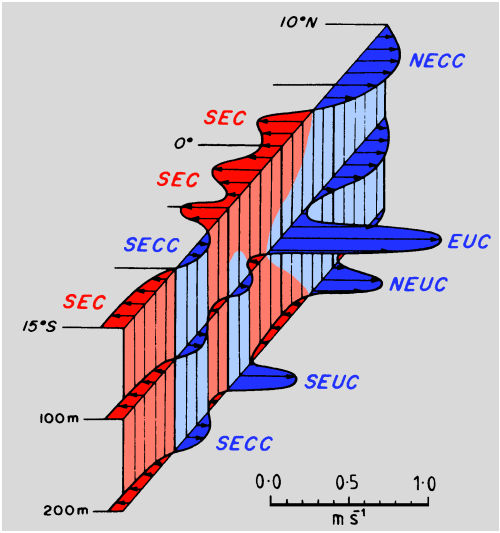

Fig. 14.3. A sketch of the structure of the equatorial current system during August. For abbreviations see text. After Peterson and Stramma (1991).

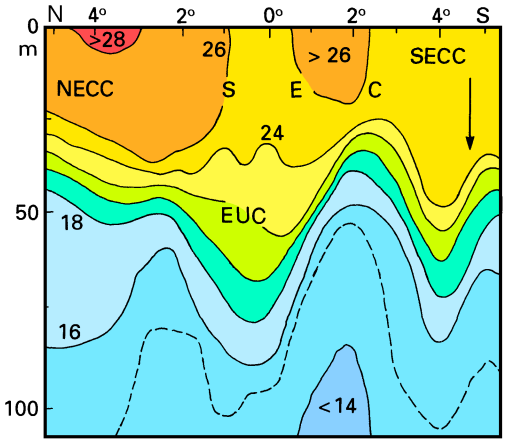

Fig. 14.4. Temperature section (°C) across the central part of the equatorial current system along 5°W. For abbreviations see text. Note the low surface temperature at the equator due to upwelling, the weakening of the thermocline in the EUC, and the poleward rise of the thermocline in the countercurrents. Adapted from Moore *et al*. (1978) .

The most conspicuous feature of the equatorial circulation is the strong cross-equatorial transport along the South American coast in the *North Brazil Current*. Of the 16 Sv carried across 30°W in the South Equatorial Current during February/March, only 4 Sv are carried south into the Brazil Current while 12 Sv cross the equator (Stramma *et al*., 1990). This is close to the estimated 15 Sv needed to feed the Deep Water source in the North Atlantic Ocean.

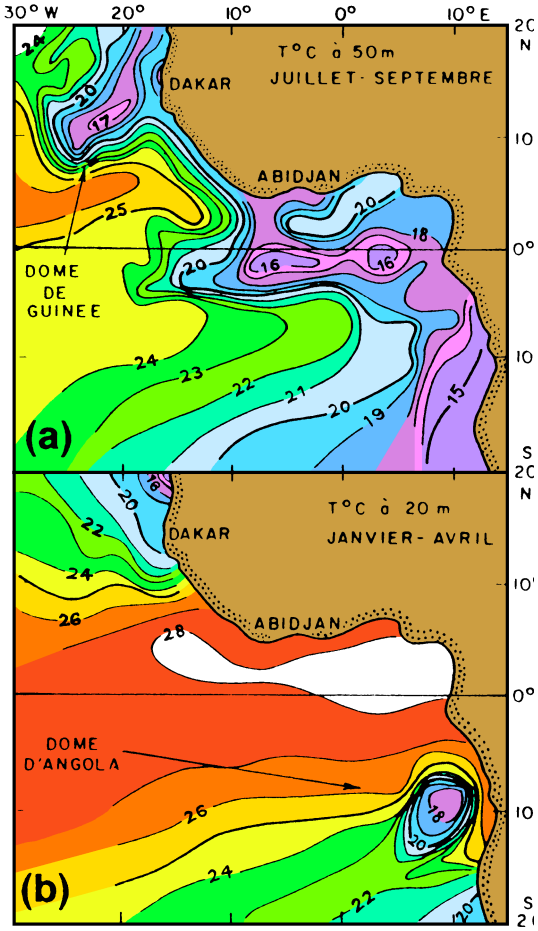

Fig. 14.6. The Angola Dome and the Guinea Dome as seen in temperature data from 20 m and 50 m depth. From Peterson and Stramma (1991)

Little exchange between hemispheres occurs in the eastern part of the equatorial zone, the termination region of all eastward flow. The South Equatorial Countercurrent turns south, driving a cyclonic gyre centred at 13°S, 4°E which extends from just below the surface to at least 300 m depth with velocities approaching 0.5 m s^{-1} near the African coast where this relatively strong subsurface flow is known as the *Angola Current* (Figure 14.2). By opposing the northward movement of the Benguela Current it creates the Angola - Benguela Front, a feature seen in the temperature of the upper 50 m and in the salinity distribution to at least 200 m depth.

The North Equatorial Countercurrent is prevented from flowing north by the east - west orientation of the coastline; it intensifies to an average 0.4 m s^{-1} along the Ivory Coast before its energy is dissipated in the Gulf of Guinea. However, some of its flow does escape north and combines with the North Equatorial Undercurrent to drive a small cyclonic gyre centred at 10°N, 22°W. A similar small gyre, centred near 10°S, 9°E and clearly distinct from the larger gyre which incorporates the Angola Current, is driven by the South

the time the flow separates from the shelf near Cape Hatteras - a distance of 1200 km downstream - it has reached a transport of 70 - 100 Sv (much more than the 30 Sv suggested by the integrated flow calculation of Chapter 4). For the next 2500 km the *Gulf Stream* proper flows across the open ocean as a free inertial jet. Its transport increases initially through inflow from the Sargasso Sea recirculation region to reach a maximum of 90 - 150 Sv near 65°W. The current then begins to lose water to the Sargasso Sea recirculation, its transport falling to 50 - 90 Sv near the Newfoundland Rise (50°W, also known as the Grand Banks). Throughout its path current speed remains large at the surface and decreases rapidly with depth, but the flow usually extends to the ocean floor (Figure 14.7).

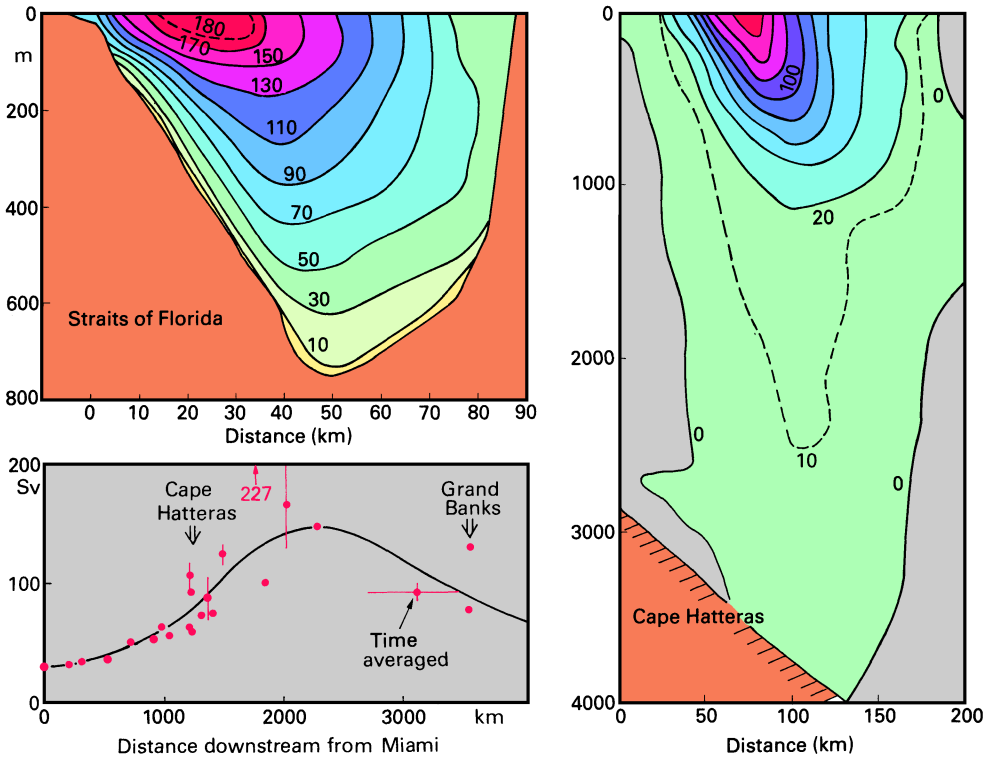

Fig. 14.7. A summary of Gulf Stream volume transports reported in the literature (based on Richardson (1985) and additional more recent data); and two sec–tions of annual mean velocity in the Florida Current and the Gulf Stream at Cape Hatteras, based on continuous vertical profiles of velocity from cruises over a 2 - 3 year period. Note the different depth and distance scales. From Leaman *et al*. (1989).

In the region east of 50°W, which is sometimes referred to as the Gulf Stream Extension, the flow branches into three distinctly different regimes (Figure 14.8). The *North Atlantic Current* continues in a northeastward direction towards Scotland and withdraws about 30 Sv

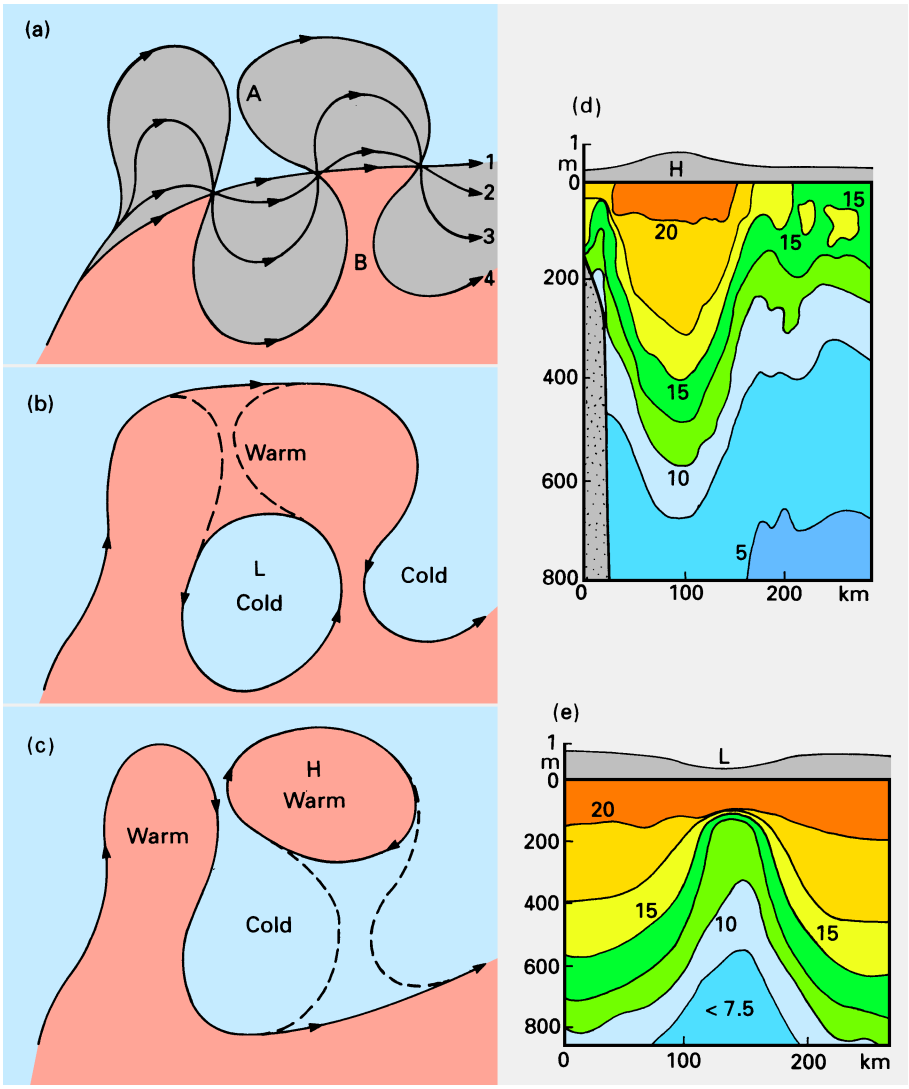

Fig. 14.9. A sketch of eddy formation in a free inertial jet and the associated hydrographic structure. (a) Path of the jet at succesive times 1 - 4. (b) A cyclonic (cold-core) ring formed after merger of the path at location *A*. The open line is the Gulf Stream path after ring formation, the closed line the ring, the dotted line the path just before eddy formation. (c) A similar representation of an anticyclonic (warm-core) ring formed if the jet merges at location *B* instead. *H* and *L* indicate high and low pressure. (d) A temperature section (°C) through an anticyclonic ring. (e) A section through a cyclonic ring. The shape of the sea surface shown in (d) and (e) was not measured but follows from Rules 1, 1a, and 2 of Chapter 3. Panels (a) - (c) show a northern hemisphere jet; the situation in the southern hemisphere is the mirror image with respect to the equator. Panels (d) and (e) apply to both hemispheres; they are adapted from Richardson (1983b).

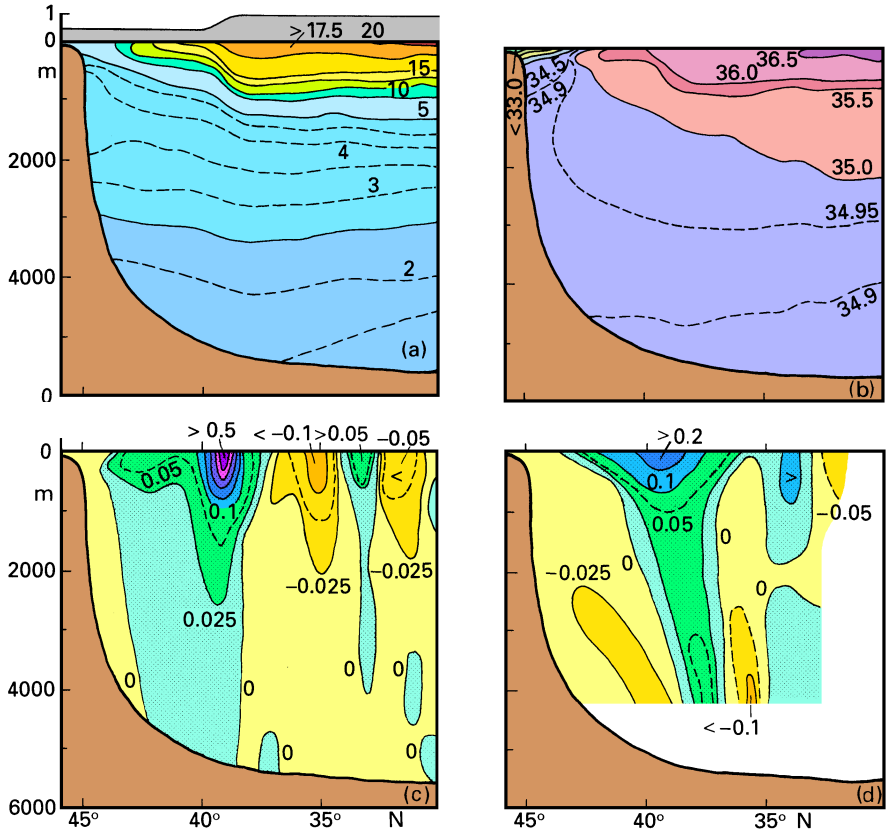

Fig. 14.12. A section through the Gulf Stream and its countercurrents across 55°W. (a) Potential temperature (°C) and sea level (m), (b) salinity, (c) geostrophic current (m s^{-1}) relative to the sea floor, (d) mean current (m s^{-1}) as derived from a combination of drifters, subsurface floats, and current meter moorings. The sections are based on data from 8 cruises between 1959 - 1983. From Richardson (1985). The shape of the sea surface as seen in more recent satellite altimeter observations is sketched above the temperature panel.

Most transport estimates for the Gulf Stream are based on geostrophic calculations which, according to our Rule 2 in Chapter 3, should be accurate to within 20%. The associated pressure gradient is maintained by a drop in sea level across the current of some 0.5 m towards the coast and, according to our Rule 1a, a corresponding thermocline rise of about 500 m. This is demonstrated by Figure 14.12 which also reveals the existence of two countercurrents, one inshore - between the continental slope and the Gulf Stream - and one offshore, as part of the long-term mean situation. Actual velocities at any particular time can be much larger, since the strong currents in the rings disappear in the mean and variability in the position of the Gulf Stream acts to reduce the peak velocity in the mean as well. Observed peak velocities usually exceed 1.5 m s^{-1}.The Gulf Stream is an important heat sink for the ocean. Net annual mean heat loss, caused by advection of cold

corresponds to a rate of increase comparable to that observed in the Gulf Stream. All these estimates are derived from geostrophic calculations with levels of no motion near or above 1500 m and therefore do not include the considerable transport of North Atlantic Deep Water below. More recent estimates which use 3000 m as level of no motion give total transports of 70 - 76 Sv near 38°S (Peterson and Stramma, 1991). The difference is larger than can be explained by the transport of Deep Water and indicates that significant recirculation must occur in the south Atlantic Ocean below 1500 m depth.

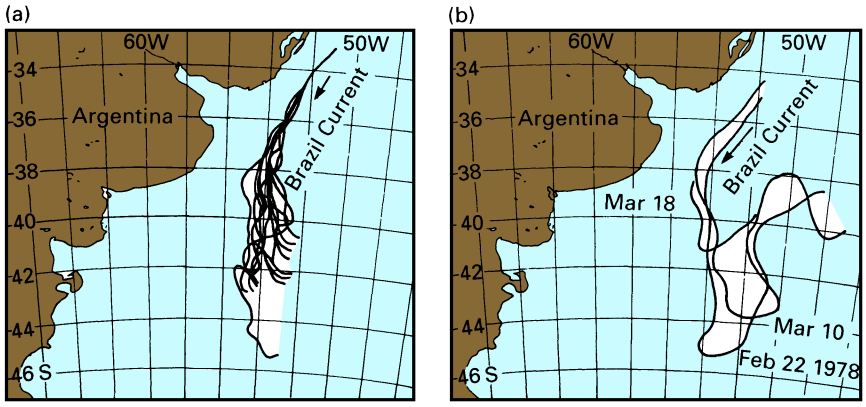

Fig. 14.14. The separation region of the Brazil Current. (a) mean position of the Brazil Current as indicated by the position of the thermal front between the Brazil and Malvinas Currents during September 1975 - April 1976; (b) a succession of three positions of the thermal front, indicating northward retreat of the Brazil Current. Two eddies formed between 22 February and 18 March; they are not included here. From Legeckis and Gordon (1982).

The Brazil Current separates from the shelf somewhere between 33 and 38°S, forming an intense front with the cold water of the *Malvinas Current*, a jet-like northward looping excursion of the Circumpolar Current also known as the Falkland Current (Figure 14.14). The separation point is more northerly during summer than winter, possibly as part of a general northward shift of the subtropical gyre in response to the more northern position of the atmospheric high pressure system (Figure 1.3) and northward movement of the contour of zero curl(τ/f) during summer (December - February). The southernmost extent of the warm Brazil Current after separation from the shelf varies between 38°S and 46°S on times scales of two months and is linked with the formation of eddies, the mechanism being very similar to that of the East Australian Current (Figure 14.15; see also Figure 8.19). Observed current speeds in Brazil Current eddies are near 0.8 m s^{-1}; transport estimates are in the vicinity of 20 Sv. Most eddies escape from the recirculation region and are swept eastward with the *South Atlantic Current*. This can be seen in the distribution of eddy energy of Figure 4.8; the large area of high eddy energy centred on 40°S, 52°W corresponds to the region of eddy formation, its tail along 48°S to the path of the decaying eddies. The two separate regions of high eddy energy east of South America also indicate that the South

Florida Current somehow, net mean movement in both the Guyana and Antilles Currents has to be toward northwest. The topic will be taken up again in the discussion of the American Mediterranean Sea in Chapter 16.

Eastern boundary currents and coastal upwelling

South of 45°N the circulation in the eastern part of the Atlantic Ocean has many similarities with that of the eastern Pacific Ocean. In the northern hemisphere the Canary Current is a broad region of moderate flow where the temperate waters of the Azores Current are converted into the subtropical water that feeds into the North Equatorial Current. In the southern hemisphere the same process occurs in the Benguela Current. Both currents are therefore characterized, when compared with currents in the western Atlantic Ocean at the same latitudes, by relatively low temperatures. As in the Pacific Ocean, equatorward winds along the eastern edge of the ocean, from Cape of Good Hope to near the equator and from Spain to about 10°N, increase the temperature contrast by adding the effect of coastal upwelling. Although the currents associated with the upwelling and those which constitute the recirculation in the subtropical gyres further offshore are dynamically independent features, the names Canary Current and Benguela Current are usually applied to both. As in other eastern ocean basins, currents in the eastern Atlantic Ocean are dominated by geostrophic eddies (an example from the vicinity of the Canary Current region is shown in Figure 4.9). Current reversals caused by passing eddies are common.

The dynamics of coastal upwelling were discussed in Chapter 8, so it is sufficient here to concentrate on regional aspects and identify the various elements of coastal upwelling systems in the Atlantic context. The *Benguela Current* upwelling system (Figure 14.16) is the stronger of the two, lowering annual mean sea surface temperatures to 14°C and less close to the coast - two degrees and more below the values seen in Figure 2.5 near the coast which indicate the effect of equatorward flow in the subtropical gyre. It is strongest in the south during spring and summer when the Trades are steady; during winter (July - September), it extends northward but becomes more intermittent because the Trades, although stronger, are interrupted by the passage of eastward travelling atmospheric lows. The width of the upwelling region coincides with the width of the shelf (200 km). Velocities in the equatorward surface flow are in the range 0.05 - 0.20 m s^{-1}; in the coastal jet near the shelf break they exceed 0.5 m s^{-1}. Poleward flow occurs on the shelf above the bottom and over the shelf break with speeds of 0.05 - 0.1 m s^{-1}, advecting oxygen-poor water from the waters off Angola; the resulting oxygen minimum along the slope can be observed over a distance of 1600 km to 30°S. The interface between equatorward surface movement and poleward flow underneath often reaches the surface on the inner shelf, producing poleward flow along the coast.

Further offshore beyond the shelf break, the equatorward surface layer flow merges with the equatorward transport of thermocline water in the Benguela Current, while poleward movement above the ocean floor continues uninterrupted, feeding into the cyclonic circulation of the deeper waters discussed in the next chapter. The dynamic independence of the recirculation in the subtropical gyre and the coastal upwelling is seen in the fact that the Benguela Current gradually leaves the coast between 30°S and 25°S, while the upwelling reaches further north to Cape Frio (18°S). Geostrophic transport in the gyre circulation

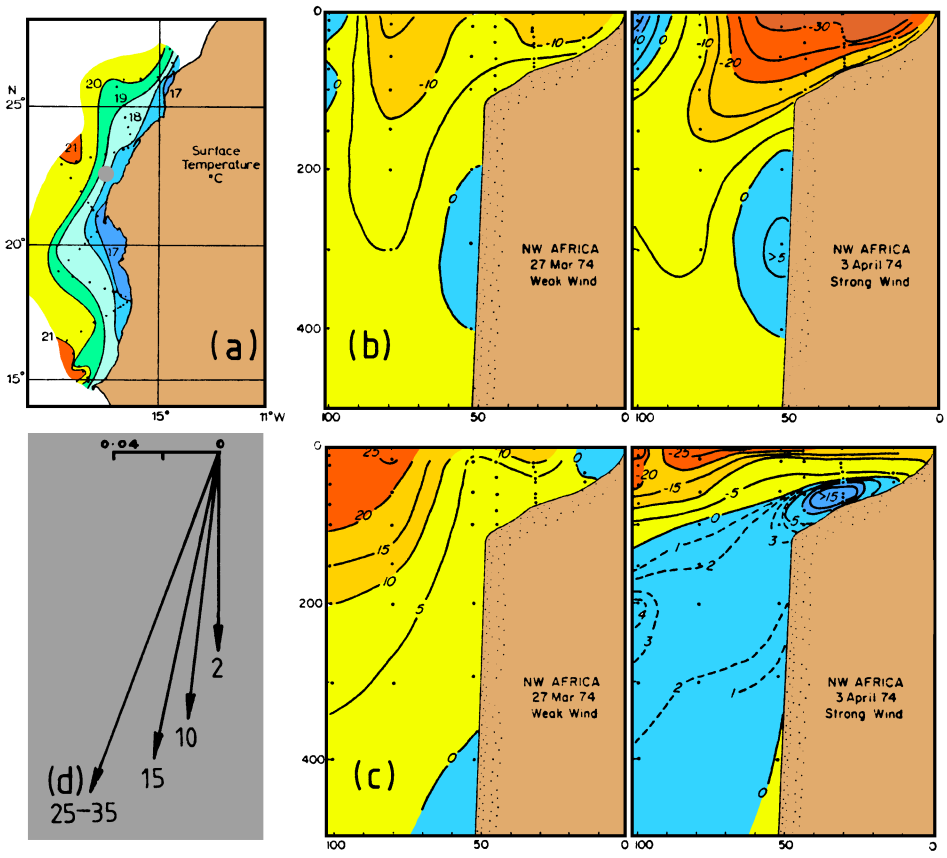

Fig. 14.17. The Canary Current upwelling system. (a) Sea surface temperature (°C) as observed in April/May 1969; (b) alongshore and (c) onshore velocities (cm s^{-1}, positive is northward and eastward) during periods of weak and strong wind, (d) observed mean velocities over a 29 day period at the position indicated by the dot in panel (a), in 74 m water depth; numbers indicate distance from the bottom. Note the alignment of the current at mid-depth with the direction of the coast, and the shoreward turning of the current as the bottom is approached. From Hughes and Barton (1974), Huyer (1976), and Tomczak and Hughes (1980).

The boundary between the westward turning Canary Current and the cyclonic circulation around the Guinea Dome marks the boundary between North Atlantic Central Water and South Atlantic Central Water, the water masses of the thermocline (which will be discussed in detail in Chapter 15). Low salinity South Atlantic Central Water is transported poleward with the surface current found along the coast of Mauritania. The undercurrent of the upwelling circulation is the continuation of this surface current. During summer when upwelling is restricted to the region north of Cap Blanc (21°N), poleward flow dominates the surface and subsurface layers south of Cap Blanc offshore and inshore; during winter it is restricted to subsurface flow along the continental slope. The depth of the undercurrent increases along its way to 300 - 600 m off Cape Bojador (27°N). In hydrographic

of course linked with significant horizontal transport of water, i.e. variations in the currents.

In the Atlantic Ocean, equatorial Kelvin waves generated off the coast of Brazil reach the Gulf of Guinea in little more than one month. They continue northward and then eastward along the African coast where they are recorded as strong regular upwelling events. For the local fishery they are of great importance, since they replenish the coastal waters with nutrients by lifting the nutrient-rich waters of the oceanic thermocline onto the shelf.

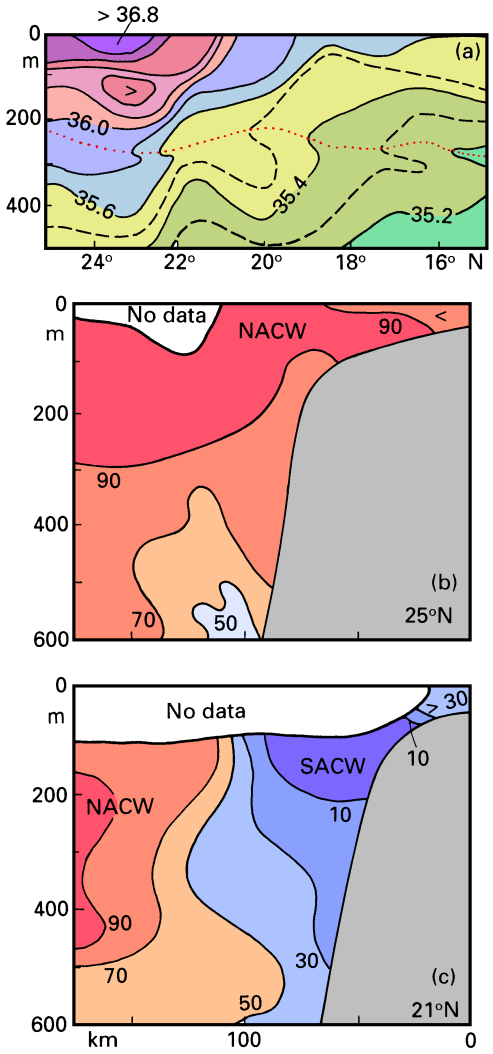

Fig. 14.19. (Left) The undercurrent of the Canary Current upwelling system as seen in hydrographic observations.

(a) a salinity section along the continental slope, showing saline North Atlantic Central Water north and low salinity South Atlantic Central Water south of 20 - 22°N and the salinity anomaly on the σ_Θ= 26.8 density surface (thin dotted line) caused by advection of SACW,

(b) distribution of water masses in a section across the shelf and slope at 25°N, expressed as % NACW content (SACW content is 100 - %NACW),

(c) a similar section at 21°N. The data for (a) were collected in April 1969, the data for (b) and (c) in February 1975. Note that the undercurrent is already well submerged at 21°N during 1969 but still close to the surface at 21°N in 1975.

Adapted from Hughes and Barton (1974) and Tomczak and Hughes (1980).